J Neurophysiol 94: 2856–2866, 2005.
First published June 29, 2005; 10.1152/jn.00802.2004.

Role of Primate Visual Area V4 in the Processing of 3-D Shape Characteristics Defined by Disparity

Jay Hegdé and David C. Van Essen
Department of Anatomy and Neurobiology, Washington University School of Medicine, St. Louis, Missouri

Submitted 5 August 2004; accepted in final form 23 June 2005

Hegdé, Jay and David C. Van Essen. Role of primate visual area V4 in the processing of 3-D shape characteristics defined by disparity. *J Neurophysiol* 94: 2856–2866, 2005. First published June 29, 2005; 10.1152/jn.00802.2004. We studied the responses of V4 neurons in awake, fixating monkeys to a diverse set of stereoscopic stimuli, including zero-order disparity (frontoparallel) stimuli, surfaces oriented in depth, and convex and concave shapes presented at various mean disparities. The responses of many V4 cells were significantly modulated across each of these stimulus subsets. In general, V4 cells were broadly tuned for zero-order disparity, and at any given disparity value, about four-fifths of the cells responded significantly above background. The response modulation by flat surfaces oriented in depth was significant for about one-quarter of cells, and the responses of about one-third of the cells were significantly modulated by convex or concave surfaces at various mean disparities. However, we encountered no cells that unambiguously distinguished a given three-dimensional (3-D) shape independent of mean disparity. Thus 3-D shapes defined by disparity are unlikely to be represented explicitly at the level of individual V4 cells. Nonetheless, V4 cells likely play an important role in the processing of 3-D shape characteristics defined by disparity as a part of a distributed network.

INTRODUCTION

Retinal images are two-dimensional (2-D) representations of the visual scene that contain no explicit information about the 3-D layout of the visual world. To infer the depth and 3-D shapes of visual objects, the visual system uses a variety of depth cues (for overviews, see Hershenson 1999; Howard and Rogers 2002; Regan 2000). Binocular (stereoscopic) disparity is a particularly salient cue that can mediate the perception of relative depth, surface orientation, curvature, and 3-D shape of visual objects (see Howard 2002; Howard and Rogers 2002; Julesz 1971; Regan 2000). Disparity cues can also be used to resolve perceptual ambiguities resulting from other depth cues (see Howard and Rogers 2002; Regan 2000).

Tuning for binocular disparity has been reported in many areas of the visual cortex (see Cumming and DeAngelis 2001; Parker and Cumming 2001). Selectivity for disparity-defined shape characteristics has also been reported in many visual areas, including disparity-defined contours in V1 and V2 and the inferotemporal cortex (Janssen et al. 2000, 2001; von der Heydt et al. 2000) and surface orientation in areas MT and V4 (Hinkle and Connor 2002; Nguyenkim and DeAngelis 2003; also see following text). Nonetheless, many aspects of how the brain encodes depth and 3-D shape from disparity cues remain unclear.

Address for reprint requests and other correspondence: D. C. Van Essen, Dept. of Anatomy and Neurobiology, Box 8108, Washington University School of Medicine, St. Louis, MO 63110 (E-mail: vanessen@brainvis.wustl.edu).

In area V4, many cells are selective for disparity (Hinkle and Connor 2001; Tanabe et al. 2004; Watanabe et al. 2002), and many are selective for relatively complex 2-D shape characteristics (Desimone and Schein 1987; Gallant et al. 1995, 1996; Pasupathy and Connor 1999, 2001). Recently, Tanabe et al. (2004) reported that many V4 cells are selective for binocularly correlated random dot stereograms relative to binocularly uncorrelated stereograms. However, the role of V4 in the processing of 3-D shape characteristics, including those defined by disparity, is not well understood. Hinkle and Connor (2002) recently reported that many V4 cells are selective for bar stimuli oriented in depth that contain both monocular and binocular shape cues (including orientation and vertical disparity). The responses of V4 cells to more complex shapes, including curved surfaces, have not been previously reported.

In the present study, we explored whether or to what extent the responses of V4 cells convey information about 3-D characteristics defined by disparity, including depth, surface orientation, and curved surfaces, using dynamic random-dot stereograms (dRDS), which are largely free of 2-D shape cues (see Cumming and DeAngelis 2001; Parker and Cumming 2001; but see Nishihara and Poggio 1982; Poggio and Poggio 1984). We find that although the responses of many individual V4 cells are modulated by the 3-D shape stimuli, none were unambiguously selective for 3-D shapes defined by disparity. Some of these results have been previously reported in abstract form (Hegdé and Van Essen 2001).

METHODS

The responses of single V4 units to stereoscopic stimuli were recorded in two awake, fixating macaque monkeys (*Macaca mulatta*). The details of the surgical and the experimental procedures have been described previously (Hegdé and Van Essen 2000, 2003). Each animal was implanted with a scleral search coil and an acrylic cranial patch using sterile surgical procedures. After the animal was fully trained in the fixation task, a small craniotomy 5 mm in diameter was made over the recording site, and a recording chamber was mounted over the craniotomy. Neurophysiological recording was carried out using epoxy-coated tungsten electrodes (A-M Systems, Carlsborg, WA) with initial impedances of 3–5 MΩ (at 10 kHz) inserted transdurally into the cortex. All animal-related procedures used in this study were reviewed and approved in advance by the Washington University Animal Studies Committee.

Stimulus set

The stimulus set consisted of 69 stimuli (Fig. 1*A*), including 21 conventional bar stimuli and 43 dRDS and five nonstereoscopic

The costs of publication of this article were defrayed in part by the payment of page charges. The article must therefore be hereby marked "*advertisement*" in accordance with 18 U.S.C. Section 1734 solely to indicate this fact.

 0022-3077/05 $8.00 Copyright © 2005 The American Physiological Society

Downloaded from jn.physiology.org on May 20, 2009

controls (not shown). Random-dot stereograms were generated using the procedure of Julesz (1971). All random-dot stimuli included a central, circularly symmetric disk presented over the classical receptive field (CRF), the disparity of which varied systematically according to the stimulus type. The central disk was surrounded by a circularly symmetric annulus, located in the nonclassical surround, in which all dots were at zero disparity for all stimuli. Disparity tuning (i.e., tuning for 0-order disparity) was sampled by 21 dRDS stimuli in which the central disk was flat and normal to the line of gaze ("normal flats") presented at 21 different disparities ranging from −1.0° (crossed, or near) to +1.0° (uncrossed, or far) in 0.1° increments. Disparity tuning was also measured in parallel using 21 bar stimuli presented within the CRF at the same set of disparities as the normal flats to help explore the interdependence of disparity tuning and 2-D shape selectivity. The disparity range of these stimuli (−1.0 to +1.0°) likely spanned the fusable range of disparities for macaques at the eccentricities used in our experiments (Howard 2002) and is typical of those used in neurophysiological studies of disparity (Cumming and DeAngelis 2001; Parker and Cumming 2001).

Selectivity for curved surfaces (i.e., second-order disparity stimuli) was explored using seven convex stimuli ("bumps") and seven concave stimuli ("dents"). For each bump or dent, the central "disk" was a 3-D Gaussian surface the SD of which was 0.25 times the diameter of the CRF. One bump and dent were presented at each of the seven mean disparities ranging from −0.75 to +0.75° in 0.25° increments. A given pair of bump and dent stimuli at a given mean disparity differed only with respect to the sign of curvature. The disparity difference between the top and bottom of any given bump (or dent) was 0.5°, symmetrically spanning the mean disparity.

Selectivity for surface orientation (i.e., first-order disparity) was explored using eight dRDS stimuli with the flat central disk tilted and slanted with respect to the line of gaze ("oriented flats") all presented at a mean disparity of 0°. The oriented flats had a tilt of 0, 90, 180, or 270° (see Fig. 1*B,* rows). The slant, defined as the angle between the line of gaze and the normal to the surface (Nalwa 1993, p. 209), was either the same as the tangent to a bump (or dent) at the point of inflection (Fig. 1*C,* ×), or half that angle ("full slants" and "half slants," respectively; Fig. 1*B*). Thus the oriented flats allowed the sensitivity to a limited range of slants and tilts to be analyzed. The five control stimuli consisted of a bar or a dRDS presented monocularly in either eye, plus an uncorrelated RDS presented binocularly.

Together, this stimulus set allowed us to explore various aspects of the neuronal representation of zero-order disparity, along with the representation of more complex shape characteristics defined by higher order variations in disparity, such as surface orientation (defined by a linear gradient of disparity) and surface curvature (defined by smooth variations in disparity gradients).

Visual stimulation and recording

Each cell's CRF was plotted, and its receptive preferences were determined using a mouse-driven bar, grating, and/or dRDS patches on the computer's monitor. For all cells recorded in the second monkey, the CRF was also plotted using custom-written plotting software, which used a small circular dRDS patch (0.25 times the estimated diameter of the CRF) as the mapping stimulus presented at vertices of a hexagonal grid centered on the putative receptive field. In general, CRFs as determined by the two techniques largely agreed with each other except for cells that were unresponsive to the dRDS patches used in automated mapping, in which case we adopted the CRFs as determined by the manual mapping.

The receptive field preferences determined during the CRF plotting were used to customize the stimulus set for the cell under study as follows. The bar stimuli had the same length, width, color, and orientation as the cell's preferred bar. For the dRDS stimuli, the color of the central disk and the color and size of the annulus were adjusted manually so as to best drive the cell. The radial size of the annulus

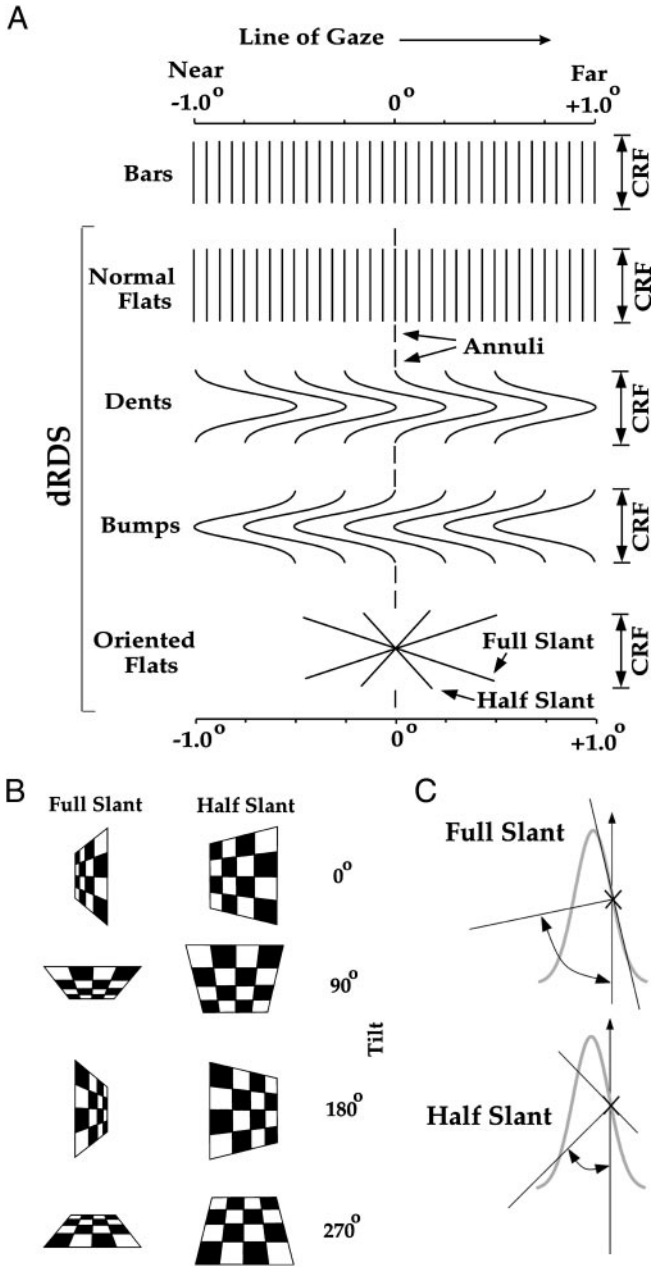

FIG. 1. The stimuli. *A*: 21 bar stimuli (*top*) and 43 dynamic random-dot stereograms (dRDS; *bottom*), consisting of normal flats, dents, bumps, and oriented flats. All stimuli are aligned relative to the same disparity scale (*top*). Note that all dRDS stimuli had an annulus at 0 disparity. Note also that the length of the bar stimuli depended on the cell's preferred bar length and was usually smaller than the diameter of the classical receptive field. On the other hand, the diameter of the classical receptive field (CRF; double arrows) determined the diameter of the dRDS stimuli and the degree of the curvature of the bump/dent stimuli and the slant of the oriented flats. The peak-to-bottom disparity difference in bump/dent stimuli was the same (0.5°) for all cells. The stimulus set also contained 5 nonstereoscopic control stimuli (not shown), including bar and random-dot stimuli presented in either eye alone plus a binocularly uncorrelated random-dot stereogram. *B*: tilts and slants of oriented flats schematically illustrated using the texture gradients of plaids. In the actual stimuli, the surface orientations and other 3-dimensional (3-D) shape characteristics of dRDS were cued solely by stereoscopic disparity. The tilt angles were fixed for all cells, but the slant angles depended on the steepness of the bump/dent stimuli as shown in *C*. See METHODS for additional details.

Downloaded from jn.physiology.org on May 20, 2009

ranged from 2 to 5°. The colors of the central disk and the annulus differed from each other for 78 of the 128 cells (61%) recorded from either animal. The preferred dRDS center color differed from the cell's preferred bar color for only 3 of the 128 cells. The stimulus color/s were chosen from a palette of eight colors (with luminances measured through active liquid crystal shutters at the center of the screen using Tektronix J17 photometer): white (6.86 cd/m^2), red (1.36 cd/m^2), green (4.93 cd/m^2), blue (0.63 cd/m^2), cyan (5.72 cd/m^2), magenta (1.98 cd/m^2), yellow (6.42 cd/m^2), and black (0 cd/m^2). All stimuli were presented against a neutral gray background (1.40 cd/m^2). The cross-talk between the two monocular images was <3% for all colors.

The size and the density of the dots varied depending on size of the receptive field so as to provide the percept of a smooth surface. The dot size ranged from 0.10 to 0.21° depending on the stimulus, although all dots in any given stimulus had the same size. The dRDS was rendered dynamically using color-lookup table animation at the refresh rate of the monitor (72 Hz), so that in any given frame, a random one-third of dots were invisible (i.e., rendered in the background color), and the remaining dots were rendered in the appropriate stimulus color. The rendered dots covered ~40–60% of the area of the monocular image at any given time. No coherent motion was apparent from one frame to the next.

Stimuli were presented dichoptically on a Sony GDM-17E11 17-in (1,280 × 1,024 pixels) noninterlaced CRT display (refresh rate, 72 Hz) fitted with NuVision (Beaverton, OR) 17SX polarized liquid-crystal shutters and viewed through passive polarized eyeglasses from a distance of 58 cm. Fixation and vergence were monitored for each eye separately using a dual scleral search coil setup (Remmel Labs, Ashland, MA). The stimuli were presented in a sequential, randomly interleaved fashion for 300–400 ms each, with a variable 300- to 400-ms interstimulus interval while the animal fixated within a window of 0.5° radius for a liquid reward. Up to six stimuli per trial were presented in this fashion. To reduce the contributions of any receptive field nonuniformities that might be present, the spatial placement of the stimuli was systematically jittered, so that a given presentation of the each stimulus was centered on one of the four points located 25% of the CRF radius away symmetrically around the CRF center. Receptive field eccentricities ranged from 1.4 to 23.9° (mean = 6.6°; n = 128). Receptive field diameters ranged from 0.9 to 19.3° (mean = 5.9°; n = 128).

Data analysis

The data were analyzed using S-Plus (Insightful, Seattle, WA), R (R Foundation for Statistical Computing, Vienna, Austria), or Matlab (Mathworks, Natick, MA) utilities and custom-written C language software. Only the data from the trials throughout which the animal maintained fixation were analyzed. The cell's evoked responses were calculated using spikes fired during a 60- to 300-ms time window after the stimulus onset; the background responses were calculated from a 100-ms time window immediately preceding the stimulus onset. Qualitatively similar results (not shown) were obtained when the time windows were customized for each cell according to the latency and the duration of the evoked responses. The response to a given stimulus was calculated as the average net firing rate across 16 repetitions (≥9 repetitions for 14 cells). A given cell was included in the analysis only if the evoked response of the cell significantly exceeded the background responses for at least one stimulus (1-tailed t-test, $P < 0.05$ after Bonferroni correction). Of the 128 cells recorded from the two animals, 119 cells (66 from *animal 1* and 53 from *animal 2*) passed this test and were included in this study.

Indices

The modulation of a given cell's response across a given subset of stimuli was measured using the corresponding *response modulation index* (RMI). To calculate the RMI for the bar stimuli (RMI_{bar}), we first determined the F ratio of the given cell's responses across all 21 bars, given by $F = MS_{between}/MS_{within}$, where $MS_{between}$ is the variance of the response across the various disparities (i.e., stimulus-to-stimulus response variance) and MS_{within} is the average noise (i.e., average trial-to-trial variance). Note that this F ratio is the same as that used by the corresponding one-way ANOVA that measures response modulation across bars. RMI_{bar} was defined as the F ratio calculated from the actual data divided by the average F ratio calculated from 10^6 randomization rounds, during each of which the spike counts from all presentations of all bars were reassigned randomly to different bars (for an overview of randomization, see Manly 1991; also see Hegdé and Van Essen 2003). The response modulation was considered statistically significant at the level of $P < 0.05$ as long as the randomized F ratio was larger than the actual F ratio in <5% of the rounds. Other RMIs similarly measured response modulations across different subsets of stimuli. RMI_{nf} measured disparity tuning across all 21 normal flats. Response modulation across the oriented flats were measured across the four oriented flats at half slant (RMI_{half}), the four oriented flats at full slant (RMI_{full}), or all eight oriented flats at either slant (RMI_{of}). For curved stimuli, response modulation was measured across the seven bumps or seven dents at various mean depths (RMI_{bump} and RMI_{dent}, respectively) or across all 14 bumps and dents (RMI_{cs}).

RMI is a more appropriate measure of response modulation (or "tuning") for V4 cells than conventional measures of tuning like tuning width or peak because V4 cells often had complex, multimodal tuning profile for disparity (see, e.g., exemplar cells in Fig. 2). RMI is also preferable over indices based on comparisons of the maximal and minimal responses (see, e.g., the disparity tuning index of Hinkle and Connor 2001, 2002) because it avoids the multiple comparison artifacts arising from selecting the responses to two stimuli out of a relatively large set of stimuli. Finally, as noted in the preceding text, RMI is an explicit measure of the signal-to-noise ratio of the responses (also see Hegdé and Van Essen 2003).

We also measured the modulation of the cell's absolute firing rates across a given subset of stimuli using two additional measures that did not take noise into account. The index σ measured the response modulation as the SD of the cell's responses across the given subset of stimuli (i.e., $\sqrt{MS_{between}}$). *Relative* σ (σ_r) was defined as $\sigma/\bar{R}$, where $\bar{R}$ is the mean response of cell across the given stimulus subset.

Population measures of disparity tuning

The average disparity tuning of V4 cells to the bar stimuli was calculated using the 84 of the 119 cells which were significantly disparity tuned for bars (RMI_{bar} analysis, $P < 0.05$). The responses of each cell to the 21 bars were normalized to a maximum of 1.0. The population average was calculated for all 21 bars by averaging the normalized responses across all 84 cells. The average disparity tuning for normal flats were was similarly calculated for the 65 cells with significant disparity tuning for these stimuli (RMI_{nf} analysis, $P < 0.05$). The population averages were also calculated separately using all 119 cells instead of using the subsets of cells with significant disparity tuning for either stimulus type (data not shown). We also calculated the rectified normalized average response of the cells to the flat stimuli. To do this, we calculated the absolute deviation of each cell's response to flat stimuli from its response to the uncorrelated random dot stimulus, i.e., we rectified the cell's responses to the flat stimuli using its response to the uncorrelated random dot stimulus as the reference (0) point. We then averaged the rectified responses across all cells as in the preceding text.

Vergence eye movements

Vergence eye movements can potentially confound the neuronal responses to stereoscopic stimuli (Cumming and Parker 1997; Masson

Downloaded from jn.physiology.org on May 20, 2009

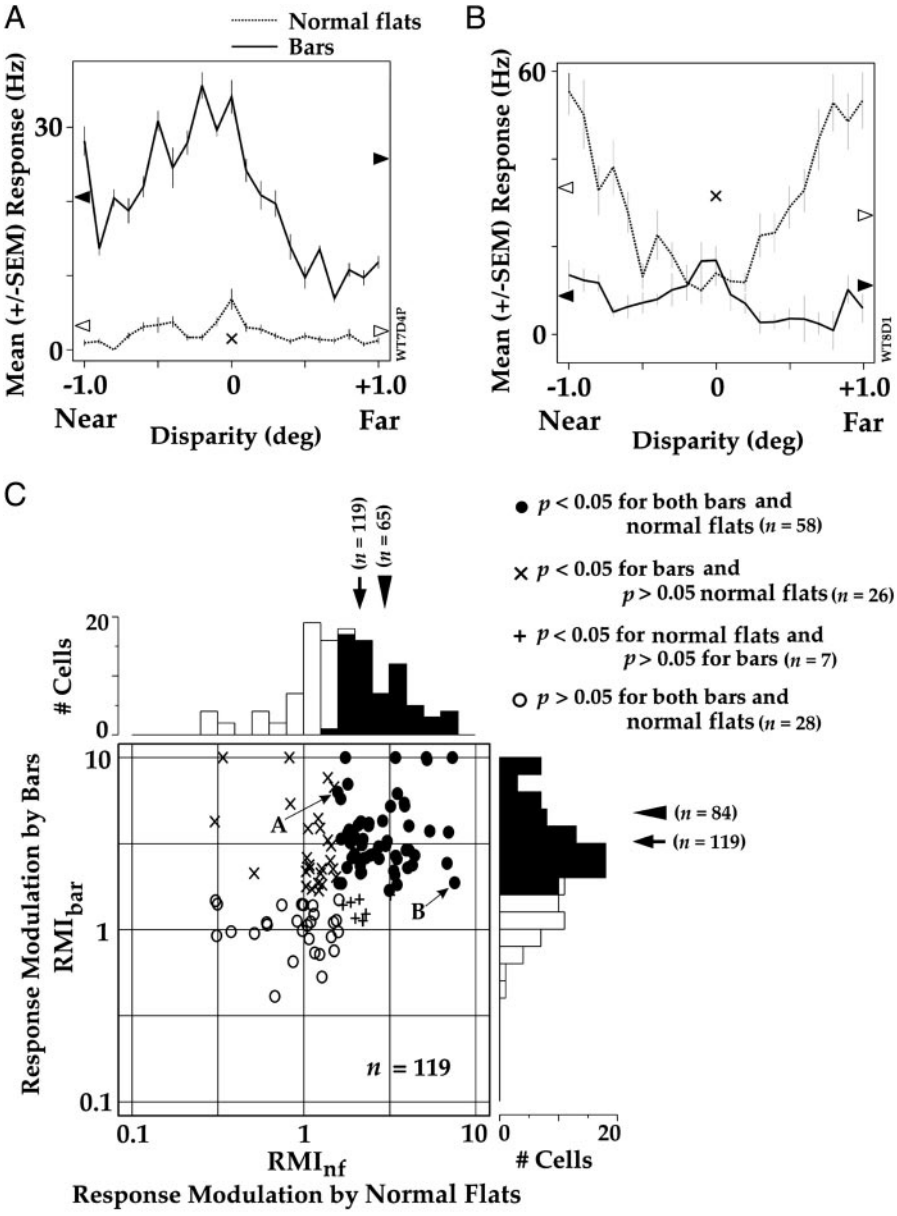

FIG. 2. Modulation of the responses of V4 cells by 0-order disparity stimuli. *A* and *B*: exemplar cells. The responses to bars presented monocularly to the left or the right eye alone are denoted by the ▶ on the left and right *y* axes, respectively. The ▷ denote the responses to the corresponding monocular dynamic random dot stimuli. ×, the response to the binocularly uncorrelated dRDS. The σ and σ_r values were 19 spikes/s, and 2.3, respectively, for the exemplar cell in *B*. For the normal flat stimuli, the σ and σ_r values were 6.64 spikes/s and 3.49, respectively, for the cell in *A;* 63.1 spikes/s and 2.12, respectively, for the cell in *B*. *C*: response modulation by bars vs. normal flats. The modulation of the responses of each V4 cell to bars and normal flats was measured using indices RMI_{bar} and RMI_{nf}, respectively, as described in METHODS. The two indices for each cell are plotted against each other in the scatterplot using log axes. The *histograms* on either axis denote the distribution of the values of the corresponding index. In this and subsequent figures, filled bars denote cells for which the value for the given index had $P < 0.05$ and □ denotes cells with $P > 0.05$. ← and ◀, the sample mean values for all cells and for cells denoted by filled bars, respectively. The relevant sample sizes *n* are indicated in parentheses where appropriate.

et al. 1997). However, vergence eye movements (calculated from 0 to 300 ms window, same as that used for calculating the evoked responses) were not a major confound in our dataset, as assessed by five different criteria. First, the average SD of the vergence angle was relatively small (0.049 for the horizontal position and 0.055 for the vertical position). Second, the vergence angles did not systematically vary with the mean disparity of the stimuli (correlation coefficient $r = 0.00001$; $P > 0.05$). Third, the vergence angles were not correlated with the neuronal responses for the corresponding stimuli ($r = -0.0001$; $P > 0.05$). Fourth, when tested using a two-way ANOVA (disparity × stimulus type) for individual cells, vergence angles varied as a function of mean disparity and stimulus type (i.e., $P < 0.05$ for the disparity and stimulus factors) for only six and eight cells, respectively, an incidence that was not above chance (binomial proportions tests, $P > 0.05$ in both cases). Finally, to determine the extent to which vergence eye movements contributed to the disparity modulation of V4 cells' responses, we compared, for each cell, the RMI value calculated using the actual responses to the 64 stereoscopic stimuli (i.e., excluding the monocular and uncorrelated dRDS stimuli) versus the RMI calculated using the average vergence angles during the same time window. The RMI values calculated using the actual responses were on average more than eight-fold higher than the corresponding RMI values calculated using vergence angles (paired 1-tailed *t*-test, $P < 0.05$).

RESULTS

Our stimuli explored the sensitivity, or tuning, of V4 cells for zero-order (i.e., uniform) disparity stimuli, as well for higher-order disparity stimuli (i.e., oriented flat surfaces and curved surfaces), which contained disparity gradients. The responses of many individual V4 cells were modulated by one or more of each of these stimulus types. We first describe the modulation of the responses of V4 cells by zero-order disparity and for higher-order disparity stimuli. A later section addresses whether or to what extent individual V4 cells are selective for a given 3-D shape over others.

Downloaded from jn.physiology.org on May 20, 2009

Tuning for zero-order disparity

DISPARITY TUNING OF INDIVIDUAL V4 CELLS. We measured disparity tuning using both bar and normal flat dRDS stimuli. Figure 2 shows the disparity tuning profile of two individual V4 cells. For the cell in Fig. 2*A*, the disparity tuning profile was tuned excitatory for both normal flats (- - -) and bars (—) with maxima near 0° but with a markedly stronger response to the bars. The cell in Fig. 2*B* showed a broad tuned-inhibitory profile for normal flat stimuli, with responses exceeding 50 spikes/s for extreme near and far stimuli. The responses to bar stimuli were generally smaller and showed a tuned excitatory peak near 0°. Although the shapes of the tuning curves for bars versus normal flats differed in each case (see following text), the disparity tuning was statistically significant for both stimulus types in both cells (1-way ANOVAs, $P < 0.05$).

For each V4 cell, we measured the strength of disparity tuning separately for the bar and normal flat stimuli using the response modulation indices RMI_{bar} and RMI_{nf}, respectively, each based on the F ratio used by the one-way ANOVA in the preceding text with additional corrections for deviations from normality (see METHODS for details). The results of this analysis are summarized in Fig. 2*C*. About three-quarters of V4 cells (91/119, 76%) were significantly tuned for disparity of bars, normal flats, or both (cells denoted by symbols, ●, ×, and + in the scatterplot, see legend for details), indicating that many V4 cells conveyed significant information about the zero-order disparity stimuli. The disparity tuning was somewhat more pronounced for bars than for normal flats, both in terms of the number of cells with significant tuning (84 cells with $P < 0.05$ for bars vs. 65 cells for normal flats; filled bars on the x- and y-axis histograms, respectively) and in terms the magnitude of the disparity tuning [mean $RMI_{bar} = 3.3 >$ mean $RMI_{nf} = 2.1$; $n = 119$ (← in the histograms); paired 1-tailed t-test, $P < 0.05$]. The degree of disparity tuning for the bar stimuli was only modestly correlated with that for normal flats across all V4 cells ($r[RMI_{nf}, RMI_{bar}] = 0.38$).

We also measured the response modulation of the cells separately across the bar and normal flat stimuli using absolute (σ) and relative (σ_r) measures of SD (see METHODS for details). For the bar stimuli, the σ value for the exemplar cell in Fig. 2*A* was 27 spikes/s, representing the SD of the responses of this cell across the 21 bar stimuli. The σ_r value this cell was 1.31, indicating that the σ value was 131% of the cell's average response across all bars. The average σ and σ_r values were 16 spikes/s and 1.85, respectively, across all 119 cells. For the normal flat stimuli, the average σ and σ_r values were 13 spikes/s and 2.8, respectively, across all 119 cells.

Together, these results indicate that the V4 cells convey disparity information for both bar and normal flat stimuli but with considerable diversity in the strength of disparity tuning for the two sets of stimuli. This analysis does not address the prominent differences in other disparity tuning parameters encountered in these and many other cells (e.g., the shape or the peak of the tuning curves), as these issues are examined in detail elsewhere (Hegdé and Van Essen 2005).

IS DISPARITY SPACE UNIFORMLY REPRESENTED IN V4? Because the issue of whether or not V4 cells represent the disparity space uniformly has important computational implications (see Abbott 1994; Field 1995; also see Richards 1970), we studied the uniformity of various response measures within the −1 to +1° range of disparities. The results of these analyses are shown in Fig. 3. The average population response across the disparity range was indistinguishable from uniform (1-way ANOVAs, $P > 0.05$) for the 84 V4 cells showing significant disparity tuning for bar stimuli (Fig. 3*A*, *top*) and for the 65 cells significantly tuned for normal flat stimuli (*bottom*).

The uniformity of the averaged responses might in principle have resulted from excitatory responses of one set of cells at a

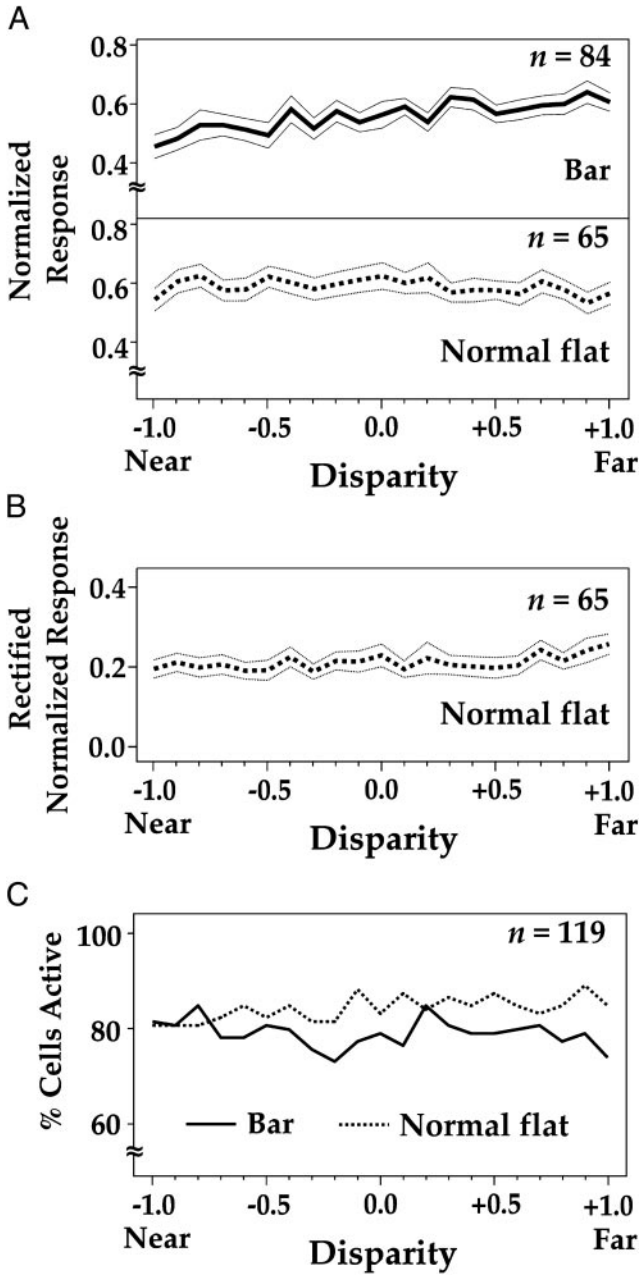

FIG. 3. Sampling of the disparity space by V4 neurons. *A*: population average response. The population averages were calculated separately for bars (*top*) and normal flats (*bottom*) using only the cells significantly tuned for either stimulus type (see METHODS for details). In either panel, thick lines, the population average; thin lines denote, ± cell-to-cell SE. *B*: population average of rectified responses to normal flats. *C*: the redundancy of disparity representation. The percentage of V4 cells that were significantly responsive above background levels at each of the 21 disparity values are shown for both the bar stimuli (solid curve) and the normal flat stimuli (dotted curve). See RESULTS for details.

Downloaded from jn.physiology.org on May 20, 2009

given disparity "canceling out" inhibitory responses of another set of cells at the same disparity. This scenario is unlikely because the cell-to-cell variance of the averaged responses was itself largely uniform across disparities (Fig. 3*A*, thin lines). Also, classical disparity tuning curves with complementary response patterns (e.g., tuned inhibitory and excitatory tuning curves) (see Poggio and Poggio 1984) were relatively rare in V4 (data not shown). Nonetheless, to further evaluate this possibility, we recalculated the population average response to normal flats using responses rectified with respect to the response to uncorrelated random dot stimulus (see METHODS). The rectified average response was also uniform across disparities (1-way ANOVA, $P > 0.05$; Fig. 3*B*). Thus the uniformity of the averaged responses cannot be attributed to a cancellation effect between excitatory and inhibitory responses.

Similar results were obtained when the population averages were calculated using all 119 cells instead of only those cells with significant disparity tuning for either stimulus type (not shown). The proportion of cells significantly responsive to either stimulus type was also uniform across disparities (Fig. 3*C*). Importantly, about three-quarters of cells on average (range, 72–86%) were significantly responsive (i.e., evoked responses > background responses) to both types of stimuli at any given disparity (paired 1-tailed *t*-test, $P < 0.05$), indicating that V4 cells code for disparity in a redundant fashion (see Field 1995). Together, these results indicate that V4 cells sample the disparity space fairly uniformly and with considerable redundancy.

Responses to higher-order shape characteristics defined by disparity

RESPONSE MODULATION BY SURFACE ORIENTATION. Our stimulus set contained eight flat surfaces oriented in depth at four tilts and two slants. For the cell shown in Fig. 4*A*, the responses were significantly modulated across tilts at both the full slant

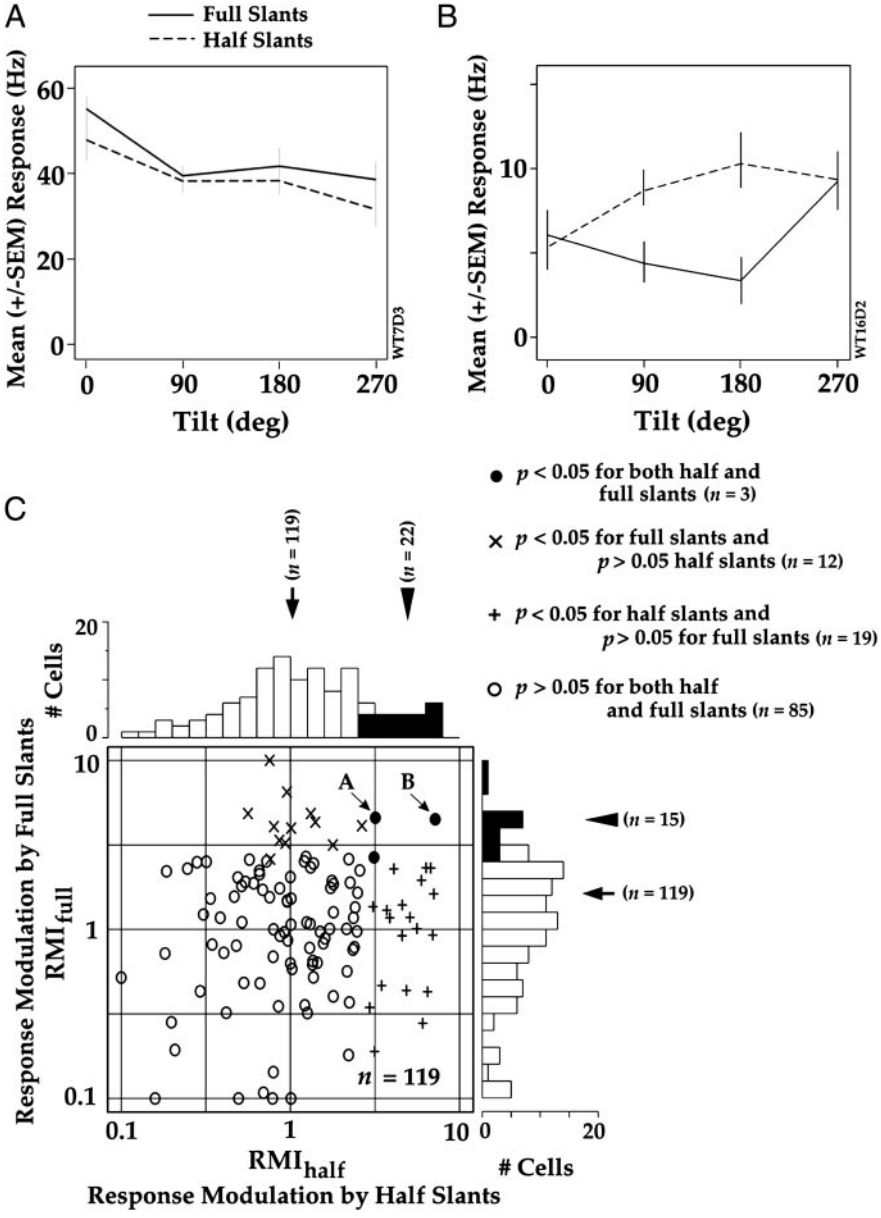

FIG. 4. Response modulation by oriented flats. *A* and *B*: exemplar cells. For full slants, the σ and σ_r values were 31 and 0.7 spikes/s, respectively, for the cell in *A*, and 15 and 0.36 spikes/s, respectively, for the cell in *B*. For half slants, the σ and σ_r values were 27 and 0.67 spikes/s, respectively, for the cell in *A*; 17 and 0.42 spikes/s, respectively, for the cell in *B*. *C*: response modulation by half vs. full slants. The modulation of the responses of each V4 cell by slanted surfaces was measured at one of 2 different tilts using indices RMI_{half} and RMI_{full} as described in METHODS; the results are plotted in this figure using the same conventions as in Fig. 2.

Downloaded from jn.physiology.org on May 20, 2009

(solid line) and the half slant (dashed line; 1-way ANOVAs, $P < 0.05$ in both cases), but the two tuning profiles were statistically indistinguishable (2-way ANOVA, slant × tilt, $P > 0.05$ for the slant and the interaction factors), indicating that this cell conveyed significant tilt information at either slant, but did not distinguish between the two slants. By comparison, for the cell shown in Fig. 4*B*, the tilt tuning was significant at either slant ($P < 0.05$, tilt factor) and differed across slants ($P < 0.05$ for the slant and the interaction factors).

We measured the tilt tuning of individual V4 cells at either slant using RMI_{full} and RMI_{half} (see METHODS). Figure 4*C* shows the distribution of RMI_{full} and the RMI_{half} values for all V4 cells. Twenty-two cells (18%) conveyed significant information about tilts at half slant and 18 cells (15%) at full slant (filled bars in the histograms on the *x* and the *y* axes, respectively). Thirty-four (29%) cells conveyed significant information about tilts at least one slant (cells denoted by symbols, ●, × and + in the scatterplot, see legend for details). The tuning profiles for tilts were significantly different at the two slants for 23 (19%) cells (2-way ANOVA, tilt × slant; interaction factor, $P < 0.05$; data not shown), indicating that these cells conveyed different tilt information at the two slants.

For full slants, the average σ and σ_r values were 11 and 1.3 spikes/s, respectively, across all 119 cells. For half slants, the average σ and σ_r values were 11 and 1.6 spikes/s, respectively, across all 119 cells.

RESPONSE MODULATION BY BUMPS AND DENTS AT DIFFERENT DEPTHS. Janssen et al. (1999, 2000) reported that many cells in IT prefer bump stimuli over dent stimuli (or vice versa) regardless of stereoscopic depth, with the response to the *least* effective bump (or dent) stimuli at least twice as large as the response to the *most* effective dent (or bump) stimulus (see, e.g., Fig. 3*C* of Janssen et al. 2000). We found no cell in area V4 that was unambiguously selective for bump or dent stimuli regardless of depth in this manner, suggesting that individual V4 cells do not explicitly represent these shapes.

Nonetheless, the responses of many V4 cells were modulated for bump and/or dent stimuli across stereoscopic depth (i.e., across mean disparities), as illustrated by the exemplar cells in Fig. 5, *A* and *B*. For both cells, the responses were modulated across various dent stimuli (1-way ANOVA, $P < 0.05$; - - -), whereas the response modulation across bump stimuli (—) was statistically insignificant ($P > 0.05$) for the cell shown in *A* but significant for the cell in *B*.

The responses of the exemplar cell in Fig. 5*A* to curved stimuli are not readily predictable from its responses to flat stimuli (· · ·). This is especially clear for the response to the bump stimulus at a mean disparity of +0.25°, which elicited a response larger than that elicited by any zero-order disparity stimuli at any depth. Furthermore, the cell's responses to the zero-order disparity stimuli did not readily predict the pattern of the cell's responses to the dent stimuli.

The responses of the cell in Fig. 5*B* to curved stimuli were qualitatively similar to the tuned inhibitory profile for flat stimuli except that the dent profile was shifted to the left and the bump profile was shifted to the right. These shifts would be expected if the disparities for the central portion of the curved stimuli dominated the responses. However, the responses to bump stimuli at mean disparities of +0.5 and +0.75° were larger than the responses to any of the zero-disparity stimuli intersected by these stimuli. To assess whether the responses of this cell were strongly dependent on stimulus position, we examined responses across the four jitter positions using a two-way ANOVA (jitter × stimulus). The jitter factor was statistically insignificant for both cells in Fig. 5, *A* and *B* ($P =$ 0.7 and 0.14, respectively), indicating that tuning profiles were not significantly dependent on jitter position. Taken together, these analyses suggest that significant nonlinear interactions contribute to the responses to bump and dent stimuli in these example cells. However, these two cells showed the most pronounced differences between the response patterns to curved stimuli versus zero-order disparity stimuli in the entire population; for the remaining cells in our sample, the two sets of response patterns were not readily distinguishable from each other.

We measured the modulation of each V4 cell to the bump and dent stimuli across various stereoscopic depths using the RMI_{bump} and RMI_{dent}, respectively (see METHODS). The results are shown in Fig. 5*C*. Across the population, the responses of 42 (35%) and 37 cells (31%) were significantly modulated for the bumps and dents across the various depths, respectively (filled bars in the histograms on the *x* and the *y* axes, respectively). Fifty-nine cells (50%) were tuned for either or both types of stimuli. The tuning profiles for bumps were significantly different from those for dents for 55 (46%) cells (2-way ANOVA, stimulus type × depth; interaction factor, $P < 0.05$; data not shown). Together, these results indicate that although individual V4 cells are not explicitly selective for the bump or dent shape per se, the responses of many V4 cells nonetheless convey information about these stimuli in a depth-dependent manner.

For the bump stimuli, the average σ and σ_r values were 13 and 1.3 spikes/s, respectively, across all 119 cells. For dents, the average σ and σ_r values were 13 and 2.7 spikes/s, respectively, across all 119 cells.

Using the ANOVA analysis of jitter position described in the preceding text, we found a statistically significant effect of jitter positions in only 9 of 119 cells (8%), an incidence not significantly greater than expected by chances (binomial proportions test, $P > 0.05$). On the one hand, these results suggest that tuning profiles are not strongly dependent on exact stimulus position as would occur if "hot spots" of disparity sensitivity were common. On the other hand, it is entirely possible that the responses to bump and dent stimuli can be accounted for by the disparity tuning for normal flat stimuli in many or most cells. Resolution of this question will entail mapping of disparity sensitivity at different spatial positions as well as different depths.

Comparison of responses to lower- versus higher-order 3-D shape characteristics

The analyses presented thus far addressed the modulation of the responses of individual V4 cells within selected subsets of stimuli. In this section, we compare the responses across different subsets of stimuli and analyze whether individual V4 cells are selective for one type of 3-D stimulus over others.

To compare the sensitivity, or "tuning" strength, of individual cells to various types of 3-D stimuli, we classified the 43 dRDS stimuli into three subclasses (see Fig. 1): 21 normal flats

Downloaded from jn.physiology.org on May 20, 2009

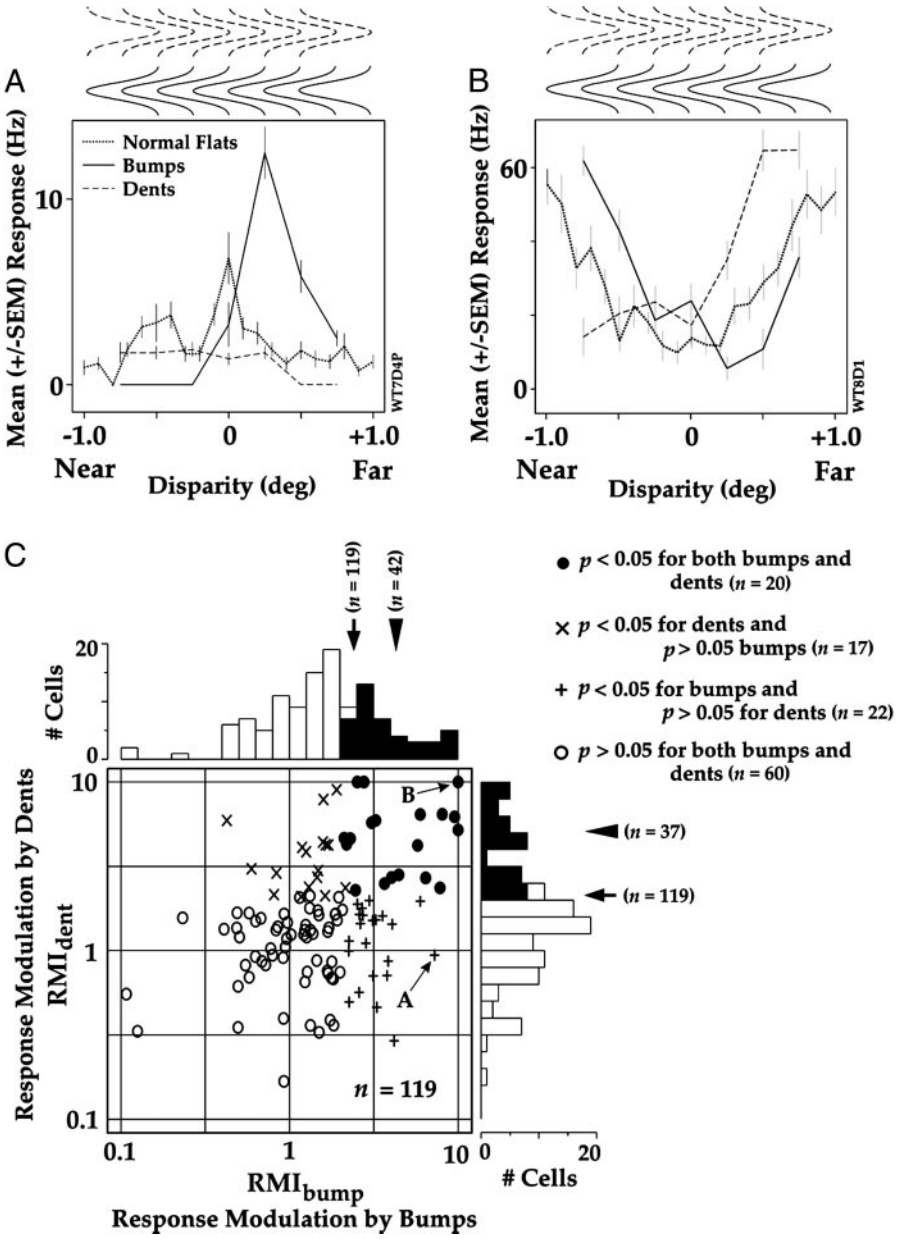

FIG. 5. Response modulation by bumps and dents at different mean stereoscopic depths. *A* and *B*: exemplar cells (the same as in Fig. 2, *A* and *B*, respectively). The responses of the cells to the normal flat stimuli are included for comparison. The bump/dent icons (*top*) illustrate the positioning of the corresponding stimuli in the disparity space. For the bump stimuli, the σ and σ_r values were 15 and 4.7 spikes/s, respectively, for the cell in *A* and 79 and 2.8 spikes/s, respectively, for the cell in *B*. For dents, the σ and σ_r values were 3.1 and 2.8 spikes/s, respectively, for the cell in *A*, 87 and 2.6 spikes/s, respectively, for the cell in *B*. *C*: response modulation by bumps vs. dents. The modulation of responses across depth was measured for the bump and dent stimuli using indices RMI_{bump} and RMI_{dent} as described in METHODS; the results are plotted in this figure using the same conventions as in Fig. 2.

(i.e., 0-order disparity stimuli), 8 oriented flats (first-order disparity stimuli), and 14 curved stimuli (second-order disparity stimuli). We then measured the response modulation across each stimulus subclass using the corresponding response modulation indices RMI_{nf}, RMI_{of} and RMI_{cs}, respectively (see METHODS).

The relative magnitudes of the three indices for all V4 cells are shown in a "sector plot" format in Fig. 6*A*, in which the deviations from the center of the plot denote a correspondingly larger RMI value for the stimulus subclass denoted by the corresponding vertex (see legend for details). For about one-third of the cells (42/119, 35%), the RMI_{nf} value was larger than either RMI_{of} or RMI_{cs} (cells in the lower right sector), indicating that the responses of these cells were modulated more by the normal flats in our stimulus set than by either of the higher-order stimulus subclasses. The RMI values were larger for the oriented flats and for the curved stimuli for about one-quarter (29/119 cells, 24%) and 4/10 (48/119, 40%) of the cells (lower left and upper sectors), respectively. However, the proportions of cells among the three sectors were indistinguishable from random given the proportions of stimuli among the three subclasses (binomial proportions test, $P > 0.05$). Also the magnitudes of the RMI values were roughly comparable for the three subclasses; the three RMI values were within a factor of two of each other for about 2/3 of the cells (78/119, 66%; cells within inner sector in Fig. 6*A*). Furthermore, for nearly half of the cells (54/119, 45%), the responses were significantly modulated across all three, or at least two of the three, subclasses (cells denoted collectively by symbols ● and *). Together, these results indicate that the response modulation in V4 was largely comparable among the zero-, first-, and second-order disparity stimuli in our stimulus set, given the caveat that the different subclasses contained unequal number of stimuli (thus varying in the statistical power of the RMI values) and that the disparity range of the oriented flats was not the same as that of the curved or normal flat stimuli for any cell (see METHODS).

Downloaded from jn.physiology.org on May 20, 2009

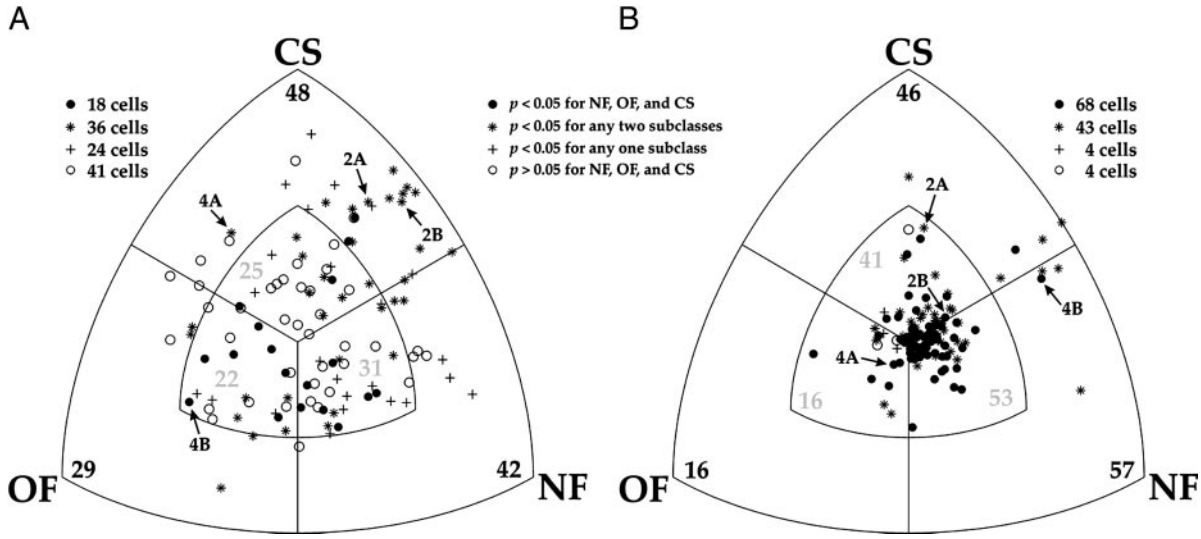

FIG. 6. Comparison of the responses to normal flats, oriented flats and curved stimuli. *A*: for each cell, the response modulation across the normal flat-, oriented flat- and curved stimuli (NF, OF, and CS, respectively) were measured using the corresponding response modulation indices (RMIs; see METHODS). Here the relative magnitudes of the 3 RMIs are plotted against each other using the sector plot method of Gallant et al. (1996). Briefly, the 3 RMI values were treated as a 3-dimensional (3-D) vector, normalized to unit length, and projected onto the surface of one sector of a unit sphere. The figure is oriented such that the origin of the coordinate system at the center, and the unit vector, where all 3 responses are equal, is projecting out of the page directly toward the viewer. Deviations from the center denote a correspondingly larger RMI value for the appropriate stimulus subclass denoted by the corresponding vertex. Within the inner sector, the 3 RMIs are within a factor of 2 of each other. Individual cells are plotted according to whether the response modulation was statistically significant ($P < 0.05$) for 1 or more of the subclasses (*inset*), and the numbers of cells denoted by the various symbols are indicated next to the plot. The black numbers inside a given sector denote the total number of cells in each sector; the gray numbers denote the number of cells within the inner triangle of each sector. Exemplar cells in Figs. 2, *A* and *B* (which were the same as those in Fig. 5, *A* and *B,* respectively), and 4, *A* and *B,* are denoted by arrows. *B*: the sector plot of the responses to the most effective stimulus from each subclass, plotted using the same conventions as in *A* except for the plotting symbols. In this panel, the plotting symbols denote whether the response to the preferred stimulus in a given subclass was significantly larger (1-tailed *t*-test, $P < 0.05$) than the responses the remaining stimuli in the given subclass for all, 2, 1, or none of the 3 subclasses.

Qualitatively similar results (not shown) were obtained when the analysis was limited to normal flats and curved stimuli, which shared the same disparity range for all cells (see METHODS).

The similarity of responses elicited by the three subclasses was even more striking when the responses of each cell to its preferred stimulus from each subclass were compared across the three subclasses (Fig. 6*B*). For about one-half of the cells (57/119, 48%), the maximal response to normal flats was larger than the maximal responses to either of the higher-order shape stimuli (lower right sector). By comparison, oriented flats and curved stimuli elicited the largest responses from 16 (13%) and 46 (39%) cells, respectively (lower left and upper sectors). This distribution of cells among the three subclasses was indistinguishable from random, given the proportions of stimuli among the three subclasses (binomial proportions test, $P > 0.05$), as was the distribution of cells for which the preference for the most effective stimulus in a given subclass was statistically significant for all three subclasses (filled circles, one-tailed *t*-test, $P < 0.05$ for all three subclasses; see legend for details). Also the three responses were within a factor of two of each other (Fig. 6*B,* inner sector) for ~9/10 of V4 cells (110/119, 92%). These results indicate that the magnitude of the response to the preferred stimulus was comparable across the three subclasses.

The data in Fig. 6*B* are replotted in Fig. 7*A* to address the question of whether a given V4 cell distinguished its most effective stimulus overall from its preferred stimuli from the other two subclasses. Each bar in this figure shows the number of cells in the corresponding sector of Fig. 6*B*. In only a single cell was the response to the most effective stimulus (a bump) significantly larger than the responses to the most effective stimuli from other subclasses (one-tailed *t*-test, $P < 0.05$ filled bar in Fig. 7*A*). When the analysis was limited only to normal flats and curved stimuli (which span the same disparity range, -1 to $+1°$, for all cells), excluding the oriented flats (the disparity range of which varied from 1 cell to the next depending on the CRF diameter; see METHODS), the results were qualitatively similar (Fig. 7*B*). The proportion of cells which preferred either subclass (64 and 55 cells, respec-

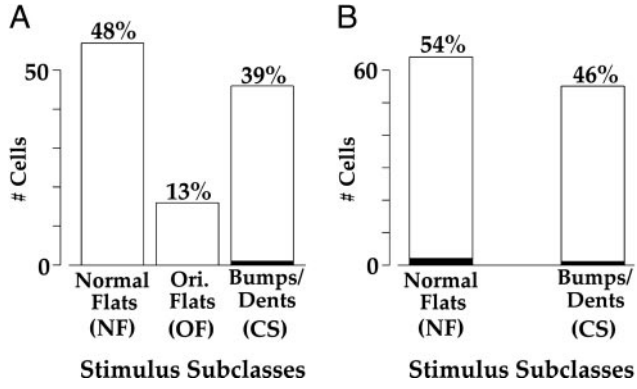

FIG. 7. Preference of individual V4 cells for subclasses of 3-D stimuli. *A*: individual V4 cells were classified into three subclasses of RDS stimuli according to whether their preferred stimulus was a normal flat, oriented flat, or a curved surface (bump/dent). The resulting distributions are shown here in barplot form. □, cells for which the response to its preferred stimulus was indistinguishable from its response to the 2nd most effective stimulus from a different subclass (one-tailed *t*-test, $P > 0.05$). The single V4 cell with $P < 0.05$ is denoted by the filled bar. *B*: the same analysis as in *A* except that oriented flat subclass was omitted from the analysis. See text for details.

Downloaded from jn.physiology.org on May 20, 2009

tively) was statistically indistinguishable from chance, given the proportion of stimuli within each subclass (binomial proportions test, $P > 0.05$). The response preference for normal flats and curved stimuli were significant for two cells and one cell, respectively (filled bars in Fig. 7*B*). With Bonferroni correction for multiple comparisons, the preference for a given subclass was significant for no V4 cell in either Fig. 7, *A* or *B* (not shown).

Together, the preceding results indicate that the three subclasses of stimuli were comparably effective for V4 cells; most V4 cells did not have a significant preference for any stimulus subclass in our stimulus set (including the normal flats) over the other two. More importantly, these results indicate that V4 cells were not unambiguously selective for their most effective 3-D shapes from any subclass.

DISCUSSION

Role of area V4 in 3-D shape processing

We found that a majority of V4 cells are significantly tuned for zero-order disparity, as measured by bars, normal flat dRDS stimuli, or both. In addition, the responses of many V4 cells are significantly modulated by dRDS surfaces at various slants and tilts and by nonplanar 3-D shape stimuli at various mean disparities. However, we found no convincing examples of consistent selectivity for a given 3-D shape stimulus in area V4. Furthermore, for the great majority of V4 cells, the responses to bump and dent stimuli were not markedly different from the average responses to zero-order disparity stimuli that spanned the same disparity range. Thus zero-order disparity selectivity may account for most or all of the responses to bump and dent stimuli for most V4 cells.

Previous studies have shown that many V4 cells are selective for complex 2-D shapes in addition to whatever stereoscopic selectivities they may have (Desimone and Schein 1987; Gallant et al. 1995; 1996; Hinkle and Connor 2002; Pasupathy and Connor 1999, 2001). Tanabe et al. (2004) reported that V4 neurons are generally more sensitive to stimulus disparity for binocularly correlated RDS compared with binocularly anticorrelated RDS, consistent with human perception and in contrast to results from area V1 (Cumming and Parker 1997). Also we have reported elsewhere (Hegdé and Van Essen 2005) that disparity tuning in many V4 cells is stimulus-dependent in that the shape of the tuning curves can differ markedly for RDS versus bar stimuli (see also Tanabe et al. 2005). Taken together, these considerations indicate that even though individual V4 neurons do not explicitly represent 3-D shapes, area V4 may nevertheless play an important role in representing 2- and 3-D shape characteristics jointly and in a distributed fashion.

Joint representation of 2- and 3-D shape characteristics is a potentially useful computational strategy. Many 2-D shape (or monocular) cues, such as motion, occlusion, and texture, provide powerful information about the 3-D layout of visual scenes. However, because any single cue to depth or 3-D shape is inherently ambiguous and insufficient to reconstruct absolute depth (Regan 2000), the brain must evaluate multiple 2- and 3-D depth cues (plus eye positions) collectively to infer the most likely 3-D configuration of any given visual scene. Neurons that represent 2- and 3-D shape characteristics concurrently, such those in area V4, may play an important role in this process. Experiments that systematically explore the interdependency of 2- and 3-D shape characteristics are needed to better understand the role of area V4 in this process.

Relation to previous studies of 3-D shape representation

Hinkle and Connor (2002) reported that many V4 cells are selective for the slants of bar stimuli, with or without surface texture, but not for stimuli the slants of which were defined solely by the disparity of surface texture. It is unclear to what extent this selectivity reflected the selectivity of the cells for 2-D cues such as perspective or texture gradients, and/or for orientation or vertical disparity. Our results are complementary, showing that the responses of many V4 cells are modulated by surface slant and tilt defined solely by horizontal disparity. Given the relatively small number of oriented flats (8) in our stimulus set, a finer-grained analysis might reveal an even higher incidence of selectivity for surface orientation, although perhaps not as prevalent or pronounced as that reported recently in area MT (Nguyenkim and DeAngelis 2003).

Janssen et al. (1999–2001) reported that many cells in area IT are selective for bump and dent RDS stimuli, in many cases regardless of the stereoscopic depth at which the stimuli were presented. By contrast, we found little evidence in V4 for such depth-invariant 3-D shape selectivity. However, rigorous comparisons between the two sets of results are difficult because the bumps and dents used by Janssen et al. (1999–2001) had 2-D outlines preferred by the cell, whereas our bump/dent stimuli all had a circular 2-D outline for all cells. Thus it is conceivable that some V4 neurons might turn out be selective for 3-D shapes independent of depth if the stimulus includes the cell's preferred 2-D outline. Further studies are needed to explore this possibility.

ACKNOWLEDGMENTS

We are grateful to Dr. Gregory C. DeAngelis for advice and help throughout this project. We thank Drs. Thomas Albright and Gene Stoner for helpful discussions.

Present address of J. Hegdé: Department of Psychology, University of Minnesota N128 Elliott Hall, 75 East River Rd, Minneapolis MN 55455-0344.

REFERENCES

Abbott LF. Decoding neuronal firing and modelling neural networks. *Q Rev Biophys* 27: 291–331, 1994.

Cumming B and DeAngelis GC. The physiology of stereopsis. *Annu Rev Neurosci* 24: 203–238, 2001.

Cumming BG and Parker AJ. Responses of primary visual cortical neurons to binocular disparity without depth perception. *Nature* 389: 280–283, 1997.

Desimone R and Schein SJ. Visual properties of neurons in area V4 of the macaque: sensitivity to stimulus form. *J Neurophysiol* 57: 835–868, 1987.

Field DJ. Visual coding, redundancy, and "feature detection." In: *The Handbook of Brain Theory and Neural Networks* edited by Arbib MA. Cambridge, MA: MIT Press, 1995, p. 1012–1016.

Gallant JL, Connor CE, Rakshit S, Lewis JW, and Van Essen DC. Neural responses to polar, hyperbolic, and Cartesian gratings in area V4 of the macaque monkey. *J Neurophysiol* 76: 2718–2739, 1996.

Gallant JL, Van Essen DC, and Nothdruft HC.Two-dimensional and three-dimensional texture processing in visual cortex of the macaque monkey. In: *Early Vision and Beyond*, edited by Papathomas TV, Chubb C, Gorea A, and Kowler E. Cambridge, MA: MIT Press, 1995, p. 89–98.

Hegdé J and Van Essen, DC. Selectivity for complex shapes in primate visual area V2. *J Neurosci* 20: RC61-66, 2000.

Hegdé J and Van Essen DC. Selectivity for 3-D shape characteristics defined by stereoscopic disparity in macaque area V4. *Soc Neurosci Abstr* 27: 165.7, 2001.

Downloaded from jn.physiology.org on May 20, 2009

Hegdé J and Van Essen DC. Strategies of shape representation in macaque visual area V2. *Vis Neurosci* 20: 313–328, 2003.
Hegdé J and Van Essen DC. Cue dependence of disparity coding in primate visual area V4. *J Neurophysiol* 93: 620–626, 2005.
Hershenson M. *Visual Space Perception.* Cambridge, MA: MIT Press, 1999.
Hinkle DA and Connor CE. Disparity tuning in macaque area V4. *Neuroreport* 12: 365–369, 2001.
Hinkle DA and Connor CE. Three-dimensional orientation tuning in macaque area V4. *Nat Neurosci* 5: 665–670, 2002.
Howard IP. *Seeing in Depth. Basic Mechanisms.* Toronto: I Porteous, 2002, vol. 1, p. 272–282.
Howard IP and Rogers BJ. *Seeing in Depth. Depth Perception.* Toronto: I Porteous, 2002, vol. 2.
Janssen P, Vogels R, Liu Y, and Orban GA. Macaque inferior temporal neurons are selective for three-dimensional boundaries and surfaces. *J Neurosci* 21: 9419–9429, 2001.
Janssen P, Vogels R, and Orban GA. Macaque inferior temporal neurons are selective for disparity-defined three-dimensional shapes. *Proc Natl Acad Sci USA* 96: 8217–8222, 1999.
Janssen P, Vogels R, and Orban GA. Three-dimensional shape coding in inferior temporal cortex. *Neuron* 27: 385–397, 2000.
Julesz B. *Foundations of Cyclopean Perception.* Chicago, IL: University of Chicago Press, 1971.
Manly BFJ. *Randomization and Monte-Carlo Methods in Biology.* New York: Chapman and Hall, 1991.
Masson GS, Busettini C, and Miles FA. Vergence eye movements in response to binocular disparity without depth perception. *Nature* 389: 283–286, 1997.
Nalwa VS. *A Guided Tour of Computer Vision.* Reading, MA: Addison-Wesley, 1993.
Nguyenkim JD and DeAngelis GC. Disparity-based coding of three-dimensional surface orientation by macaque middle temporal area neurons. *J Neurosci* 23: 7117–7128, 2003.
Nishihara HK and Poggio T. Hidden cues in random-line stereograms. *Nature* 300: 347–349, 1982.
Parker AJ and Cumming BG. Cortical mechanisms of binocular stereoscopic vision. *Prog Brain Res* 134: 205–216, 2001.
Pasupathy A and Connor CE. Responses to contour features in macaque area V4. *J Neurophysiol* 82: 2490–2502, 1999.
Pasupathy A and Connor CE. Shape representation in area V4: Position-specific tuning for boundary conformation. *J Neurophysiol* 86: 2505–2519, 2001.
Poggio GF and Poggio T. The analysis of stereopsis. *Annu Rev Neurosci* 7: 379–412, 1984.
Regan D. *Human Perception of Objects.* Sunderland, MA: Sinauer, 2000.
Richards W. Stereopsis and stereoblindness. *Exp Brain Res* 10: 380–388, 1970.
Tanabe S, Umeda K, and Fujita I. Rejection of false matches for binocular correspondence in macaque visual cortical area V4. *J Neurosci* 24: 8170–8180, 2004.
Tanabe S, Doi T, Umeda K, and Fujita I. Disparity-tuning characteristics of neuronal responses to dynamic random-dot stereograms in macaque visual-area V4. *J Neurophysiol* 94: 2683–2699, 2005.
von der Heydt R, Zhou H, and Friedman HS. Representation of stereoscopic edges in monkey visual cortex. *Vision Res* 40: 1955–1967, 2000.
Watanabe M, Tanaka H, Uka T, and Fujita I. Disparity-selective neurons in area V4 of macaque monkeys. *J Neurophysiol* 87: 1960–1973, 2002.

Downloaded from jn.physiology.org on May 20, 2009